Electronic Supplementary Material (ESI) for RSC Advances.
This journal is © The Royal Society of Chemistry 2022

Electronic Supplementary Information

Freshness monitoring of raw fish by detecting biogenic amines using a gold nanoparticle-based colorimetric sensor array

Linlin Du [a, ‡], Yijia Lao [a, ‡], Yui Sasaki [b], Xiaojun Lyu [b], Peng Gao [a], Si Wu [a], Tsuyoshi Minami [b,*] and Yuanli Liu [a,*]

[a] Guangxi Key Laboratory of Optical and Electronic Materials and Devices, College of Materials Science and Engineering, Guilin University of Technology, Guilin, 541004, China

Corresponding author: lyuanli@glut.edu.cn

[b] Institute of Industrial Science, The University of Tokyo, Tokyo, 153-8505, Japan

Corresponding author: tminami@iis.u-tokyo.ac.jp

[‡]These authors contributed equally to this work.

Contents

1. Characterization of AuNPs obtained by DS or IS

1-1. Extinction measurements

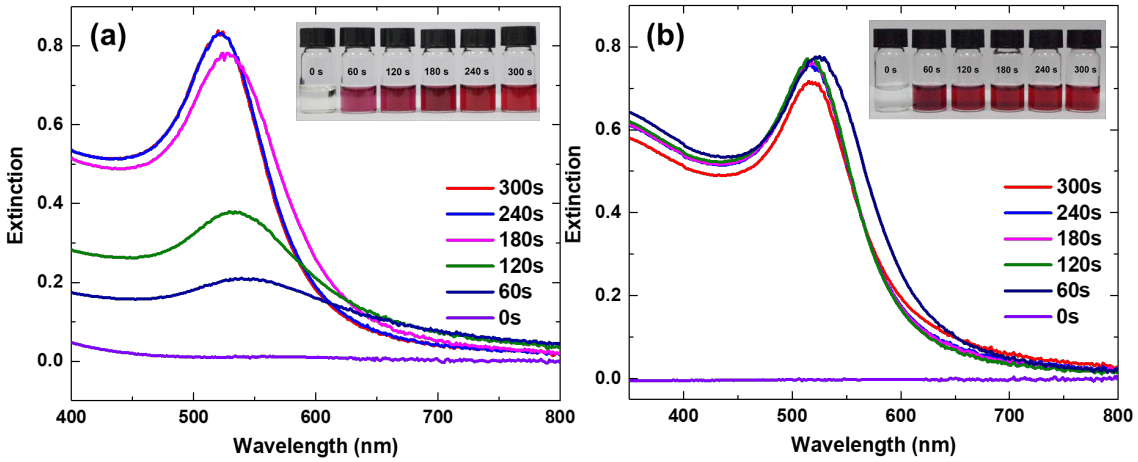

Fig. S1 Extinction spectral changes of AuNPs obtained by (a) DS or (b) IS at various times for the reaction. The evaluation was carried out in H_2O at 25 °C.

1-2. Transmission electron microscope (TEM)

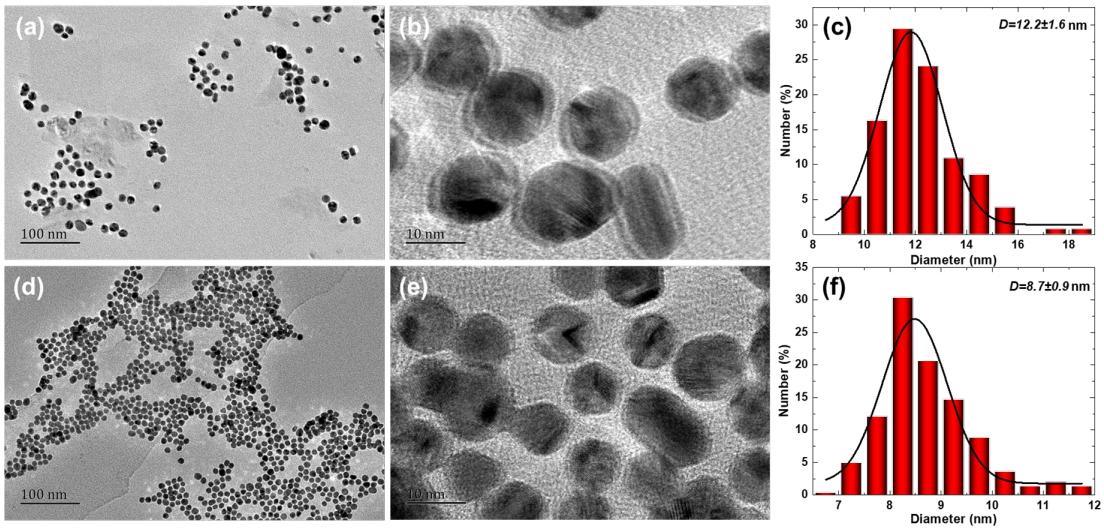

Fig. S2 TEM images and particle size distribution of AuNPs prepared via different synthesis method [DS-AuNPs (a-c) and IS-AuNPs (d-f)].

2. Characterization of AuNP-based chemosensors

2-1. Extinction measurements

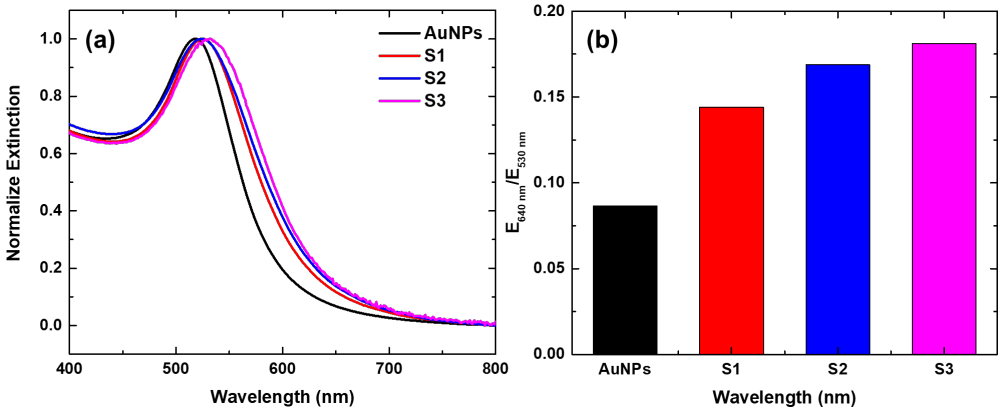

Fig. S3 (a) Extinction spectra of untreated AuNPs (black line), and the functionalized AuNPs (**S1**: red line, **S2**: blue line, and **S3**: pink line) and (b) extinction at $E_{640\ nm}/E_{530\ nm}$. The evaluation was carried out in a MES buffer solution (10 mM) at pH 5.5 at 25 °C. [**S1**–**S3**] = 1.2 ×10^{-4} g mL^{-1}.

2-2. FT-IR measurements

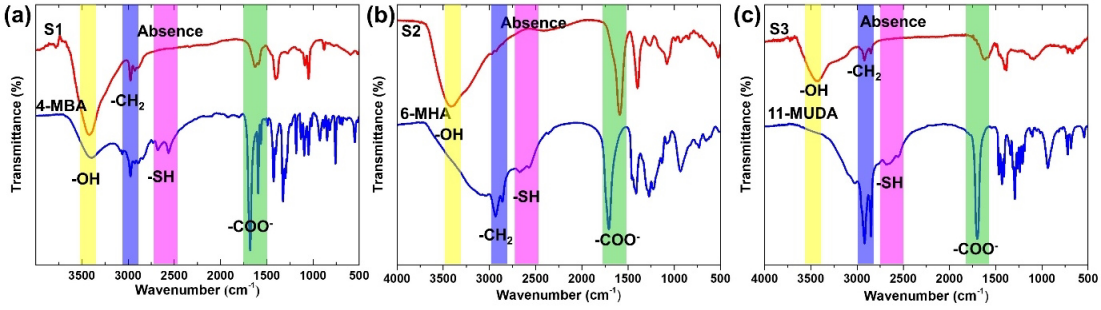

Fig. S4 FT-IR (KBr pellet) spectra of (a) **S1** (red) and 4-mercaptobenzoic acid (4-MBA) (blue), (b) **S2** (red) and 6-mercaptohexanoic acid (6-MHA) (blue), and (c) **S3** (red) and 11-mercaptoundecanoic acid (11-MUDA) (blue).

2-3. Thermal gravimetric analysis (TGA)

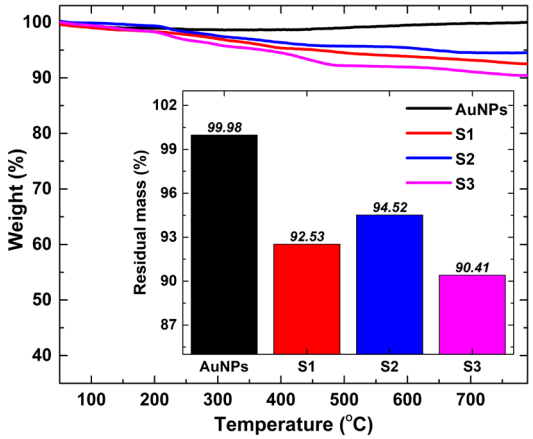

Fig. S5 TGA profile of untreated AuNPs (black line), and the functionalized AuNPs (**S1**: red line, **S2**: blue line, and **S3**: pink line). Inset represents the char yield.

2-4. X-ray photoelectron spectroscopy (XPS)

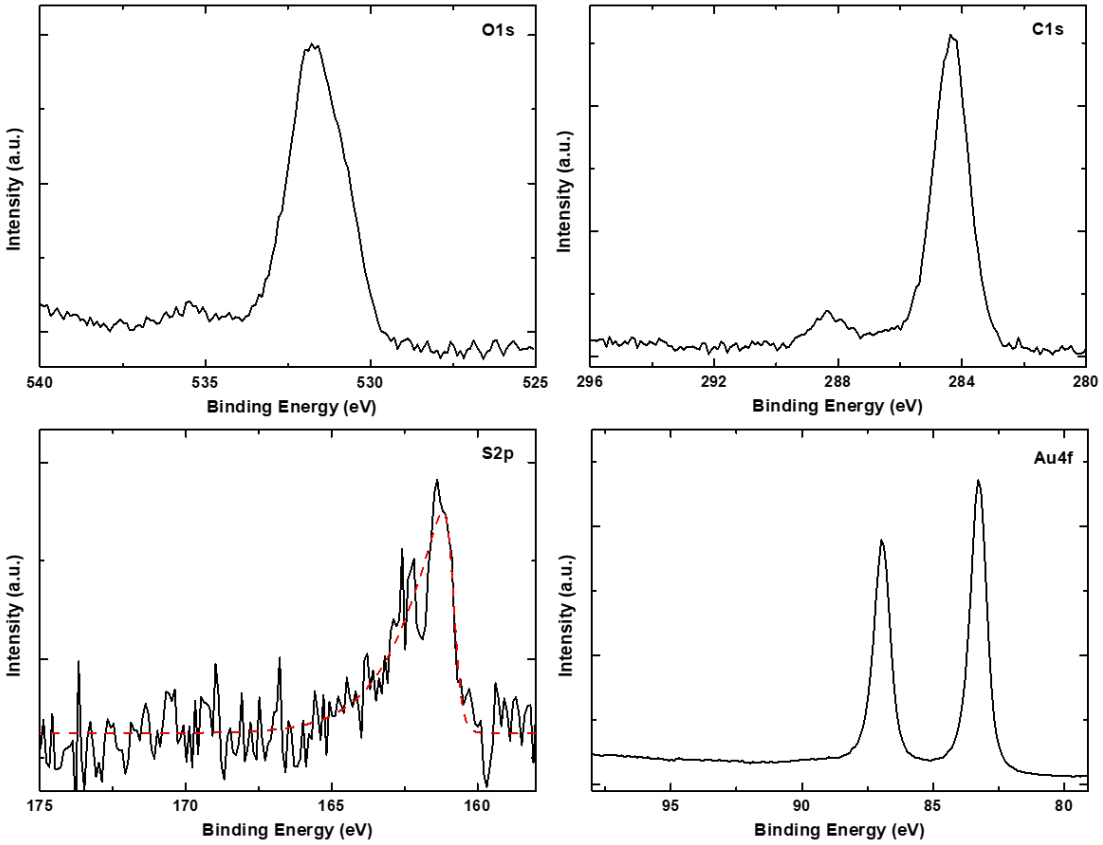

Fig. S6 XPS data of O1s, C1s, S2p, and Au4f peaks originating from **S3**.

2-5. High angle annular dark-field scanning transmission electron microscopy (HAADF-STEM)

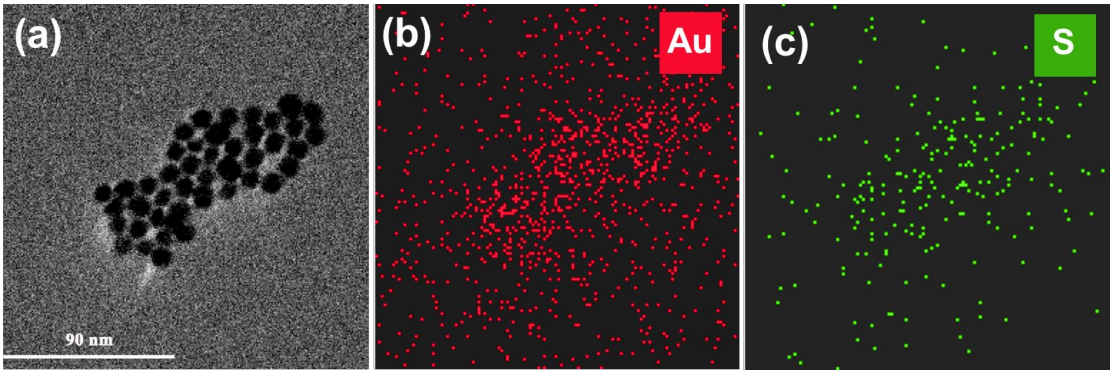

Fig. S7 (a) HAADF-STEM and EDX-mapping images of (b) Au and (c) S originating from **S3**.

2-6. Dynamic light scattering (DLS)

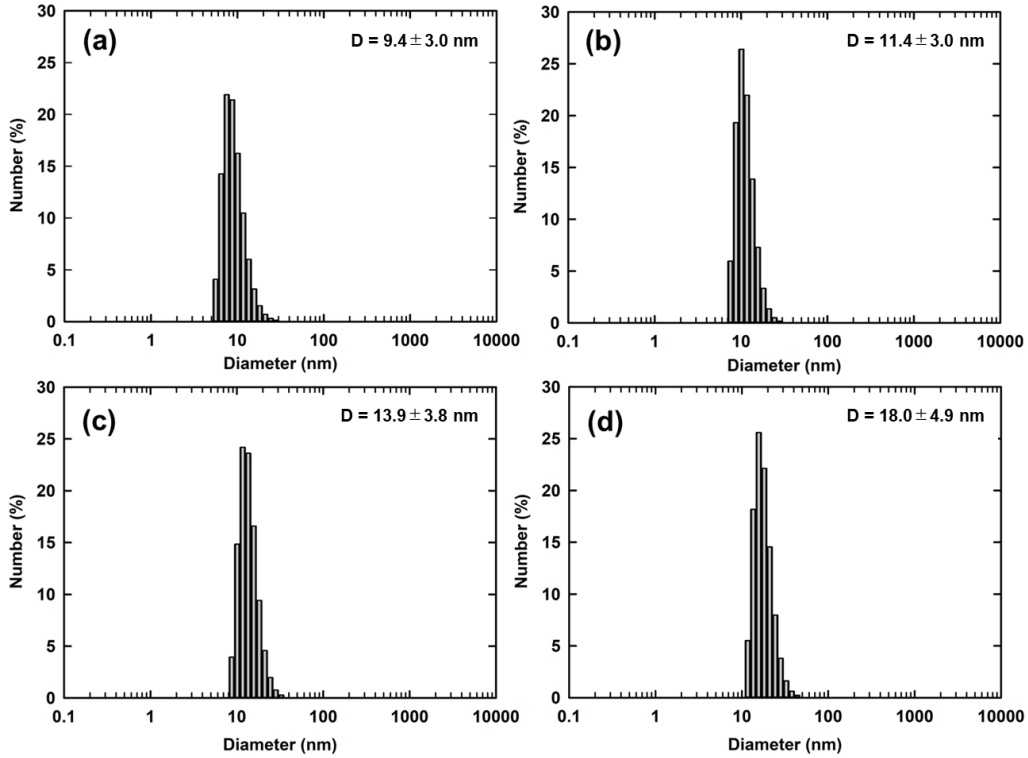

Fig. S8 The DLS diameter histograms of (a) untreated AuNPs, (b) **S1**, (c) **S2** and (d) **S3**.

2-7. Transmission electron microscope (TEM)

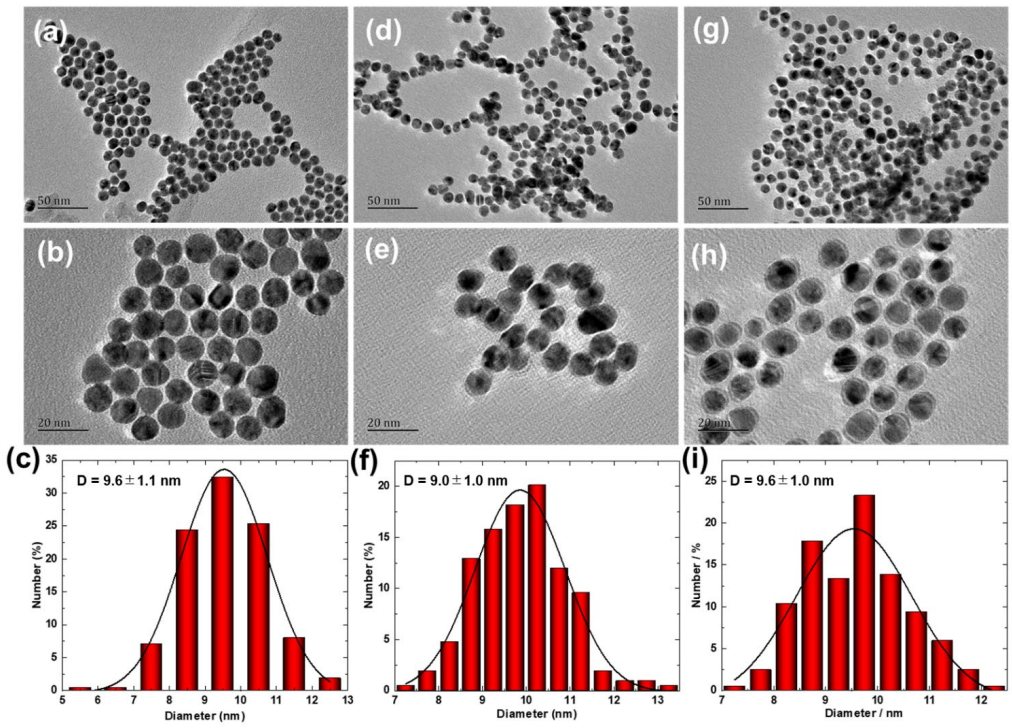

Fig. S9 Top: Morphological (TEM) characterization of AuNP-based chemosensors [**S1** (a, b), **S2** (d, e), and **S3** (g, h)]. Bottom: the results of the size distribution measurements for (c) **S1**, (f) **S2**, and (i) **S3**.

2-8. Zeta potential

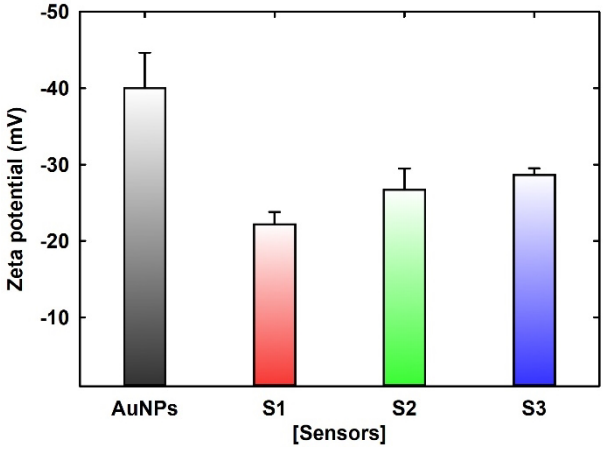

Fig. S10 Zeta potential histograms of untreated AuNPs and the functionalized AuNPs (**S1**, **S2**, and **S3**).

3. Extinction titrations

3-1. pH titration

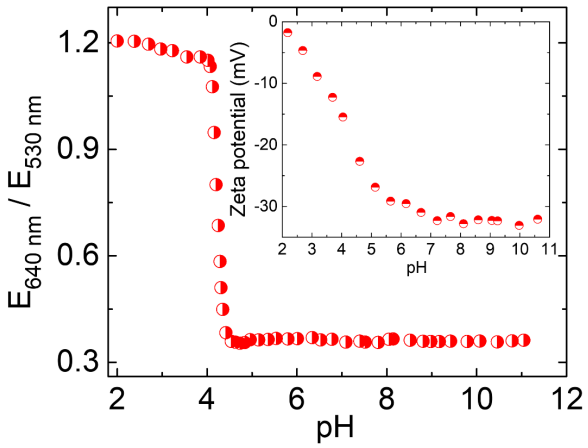

Fig. S11 The pH dependency of the colorimetric response of **S2** (1.2×10^{-4} g mL^{-1}) at $E_{640\ nm}/E_{530\ nm}$. Inset: ζ-potential values of **S2** at various pH conditions. The pH titration was carried out in the aqueous solution between pH 2.0 and pH 11 at 25 °C.

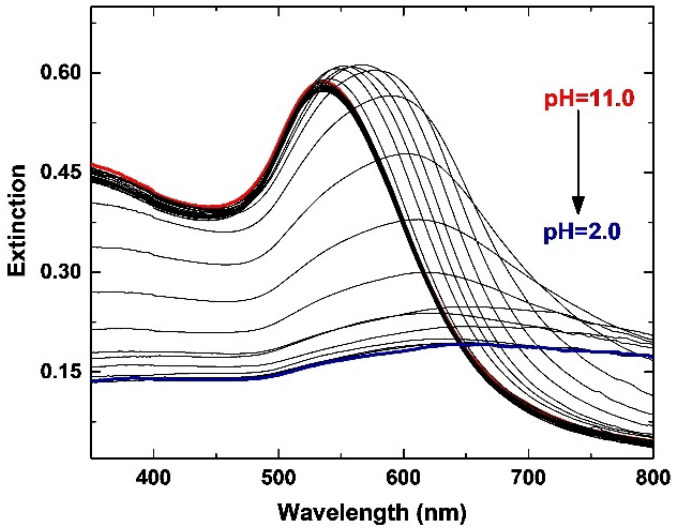

Fig. S12 Changes of extinction spectra of **S2** (1.2×10^{-4} g mL^{-1}) with dependence on pH changes. The pH titration was carried out in an aqueous solution at pH 2.0–11.0 at 25 °C.

3-2. Time-dependency

The time-dependent colorimetric changes of **S2** upon the addition of histamine were investigated by extinction spectral measurements. As shown in Fig. S13, the drastic extinction spectral shift of **S2** was observed by adding histamine within 2 min, which reached the maximum extinction intensity. After this period, the extinction spectra redshifted time-dependently and displayed an increase of the baseline accompanied with precipitation. The too-long incubation time caused precipitation, and subsequent strong Rayleigh scattering was not negligible. Thus, we decided to set 2 min as the incubation time to obtain spectral changes derived from the LSPR phenomena rather than Rayleigh scattering.

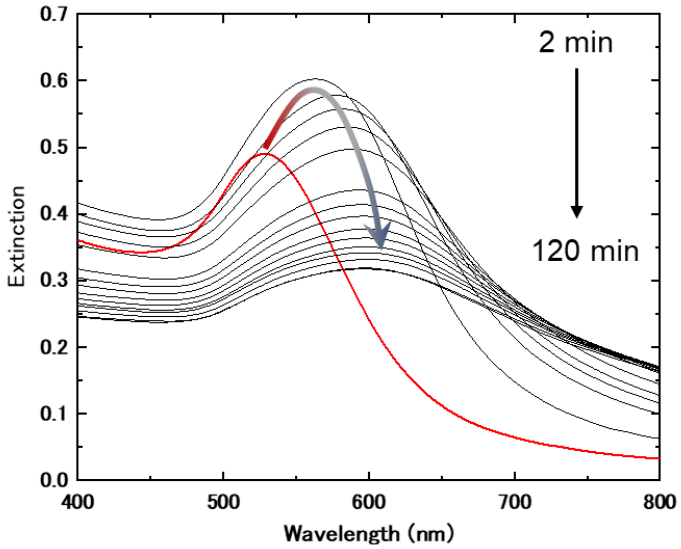

Fig. S13 Time-dependency of extinction spectra of **S2** (1.2×10^{-4} g mL^{-1}) with histamine (1.0 mM) in a MES buffer solution (10 mM) at pH 5.5 at 25 °C. The red line represents the spectrum of **S2** and the black lines represent the spectra of **S2** with histamine. The time-dependent spectral changes were recorded after 2, 6, 10, 15, 20, 30, 40, 50, 60, 70, 80, 90, 100, 110, and 120 min.

3-3. Examples of amine detection

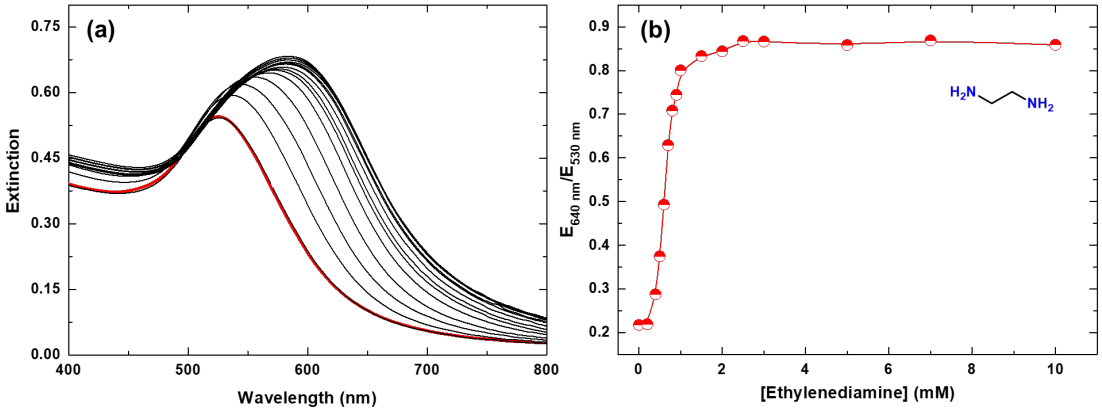

Fig. S14 (a) The extinction spectra and (b) changes in the extinction ratio ($E_{640\ nm}/E_{530\ nm}$) of **S2** (1.2 $\times10^{-4}$ g mL^{-1}) upon the addition of ethyldiamine in a MES buffer solution (10 mM) at pH 5.5 at 25 °C. [Ethyldiamine] = 0 − 10 mM.

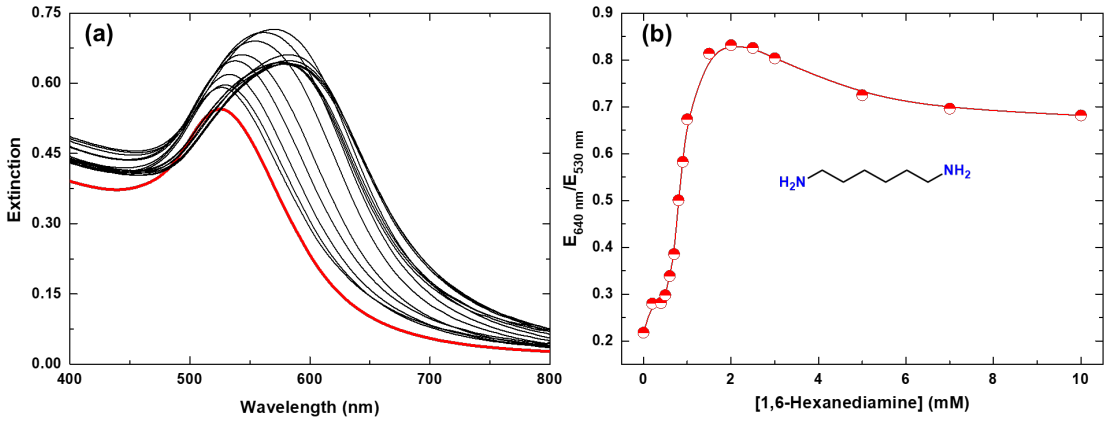

Fig. S15 (a) The extinction spectra and (b) changes in the extinction ratio ($E_{640\ nm}/E_{530\ nm}$) of **S2** (1.2 $\times10^{-4}$ g mL^{-1}) upon the addition of 1,6-hexanediamine in a MES buffer solution (10 mM) at pH 5.5 at 25 °C. [1,6-Hexanediamine] = 0 − 10 mM.

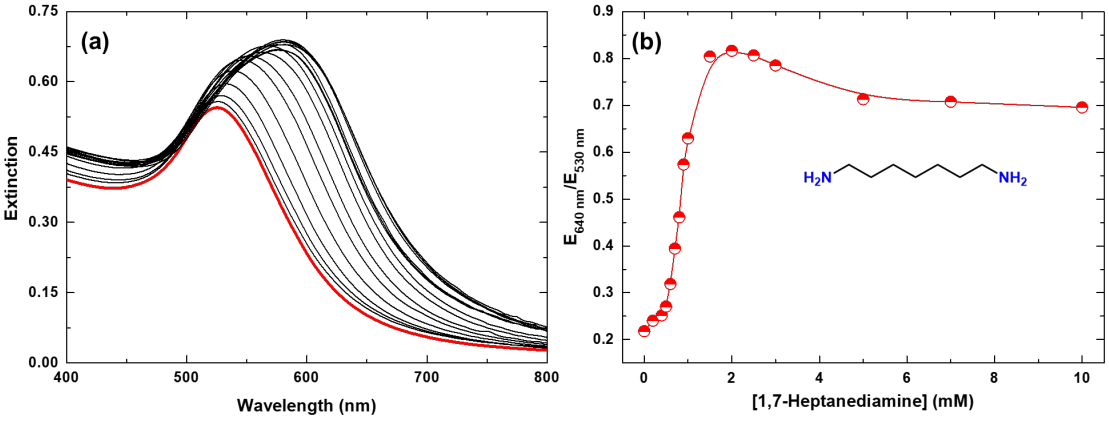

Fig. S16 (a) The extinction spectra and (b) changes in the extinction ratio ($E_{640\ nm}/E_{530\ nm}$) of **S2** (1.2 $\times10^{-4}$ g mL^{-1}) upon the addition of 1,7-heptanediamine in a MES buffer solution (10 mM) at pH 5.5 at 25 °C. [1,7-Heptanediamine] = 0 − 10 mM.

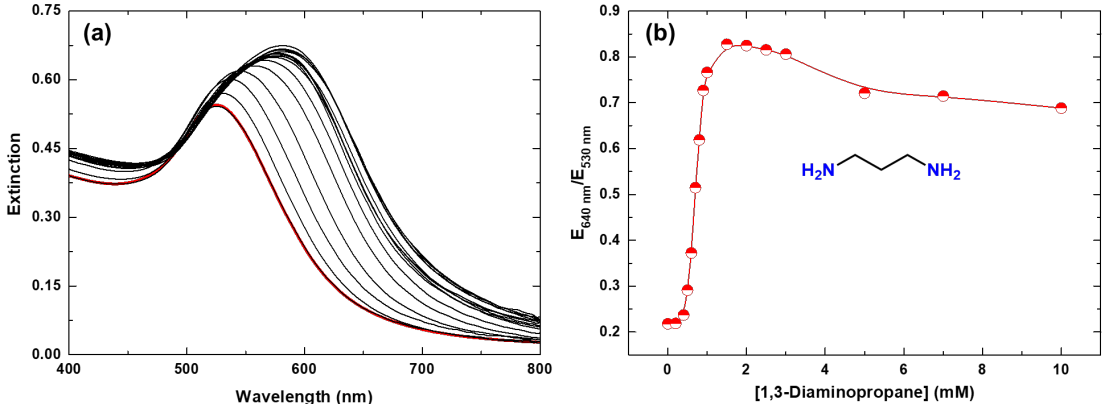

Fig. S17 (a) The extinction spectra and (b) changes in the extinction ratio ($E_{640\ nm}/E_{530\ nm}$) of **S2** (1.2 $\times10^{-4}$ g mL^{-1}) upon the addition of 1,3-diaminopropane in a MES buffer solution (10 mM) at pH 5.5 at 25 °C. [1,3-Diaminopropane] = 0 − 10 mM.

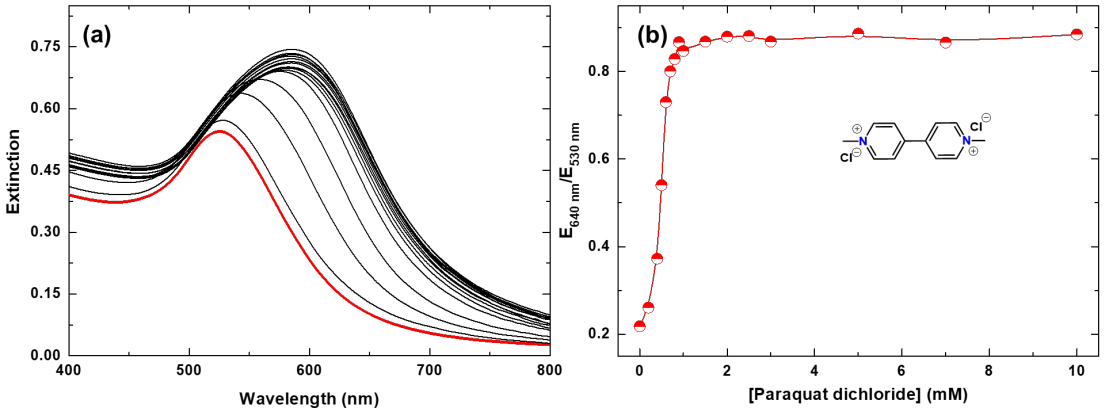

Fig. S18 (a) The extinction spectra and (b) changes in the extinction ratio ($E_{640\ nm}/E_{530\ nm}$) of **S2** (1.2 $\times10^{-4}$ g mL^{-1}) upon the addition of paraquat dichloride in a MES buffer solution (10 mM) at pH 5.5 at 25 °C. [Paraquat dichloride] = 0 − 10 mM.

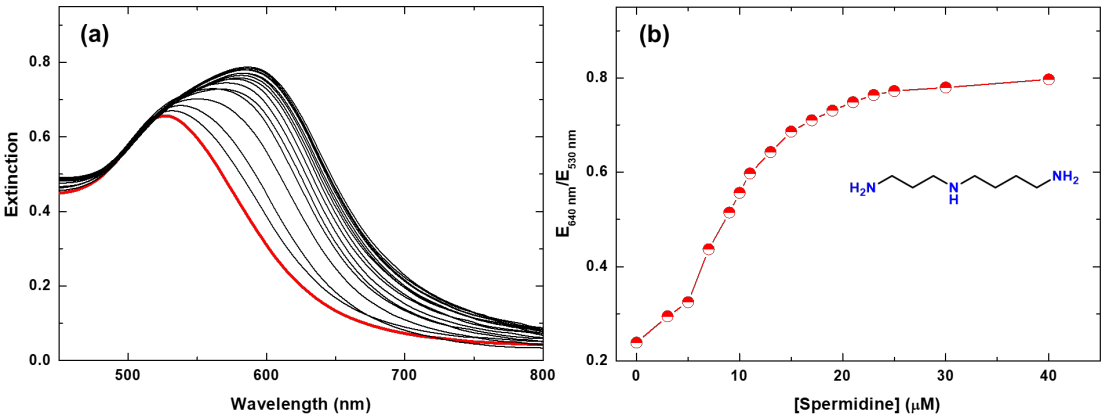

Fig. S19 (a) The extinction spectra and (b) changes in the extinction ratio ($E_{640\ nm}/E_{530\ nm}$) of **S2** (1.2 $\times10^{-4}$ g mL^{-1}) upon the addition of spermidine in a MES buffer solution (10 mM) at pH 5.5 at 25 °C. [Spermidine] = 0 − 40 μM.

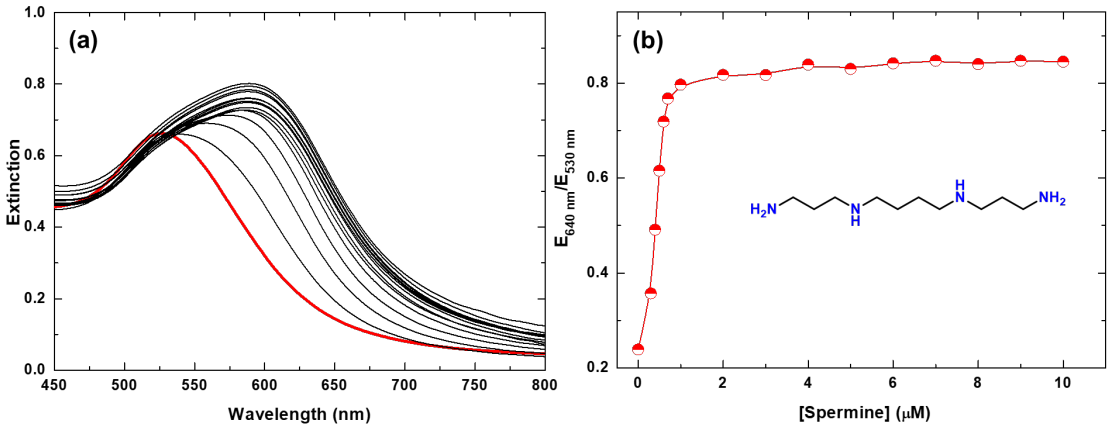

Fig. S20 (a) The extinction spectra and (b) changes in the extinction ratio ($E_{640\ nm}/E_{530\ nm}$) of **S2** (1.2 $\times10^{-4}$ g mL^{-1}) upon the addition of spermine in a MES buffer solution (10 mM) at pH 5.5 at 25 °C. [Spermine] = 0 − 10 μM.

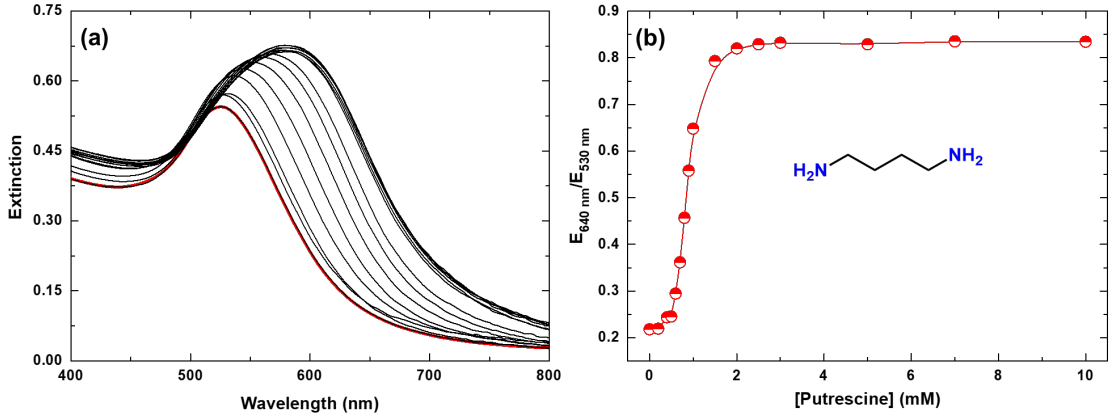

Fig. S21 (a) The extinction spectra and (b) changes in the extinction ratio ($E_{640\ nm}/E_{530\ nm}$) of **S2** (1.2 $\times10^{-4}$ g mL^{-1}) upon the addition of putrescine in a MES buffer solution (10 mM) at pH 5.5 at 25 °C. [Putrescine] = 0 − 10 mM.

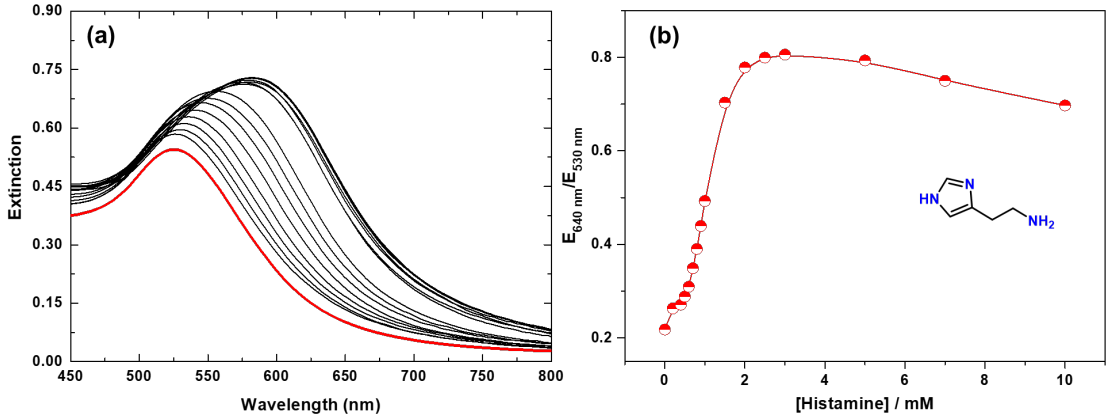

Fig. S22 (a) The extinction spectra and (b) changes in the extinction ratio ($E_{640\ nm}/E_{530\ nm}$) of **S2** (1.2 $\times10^{-4}$ g mL^{-1}) upon the addition of histamine in a MES buffer solution (10 mM) at pH 5.5 at 25 °C. [Histamine] = 0 − 10 mM.

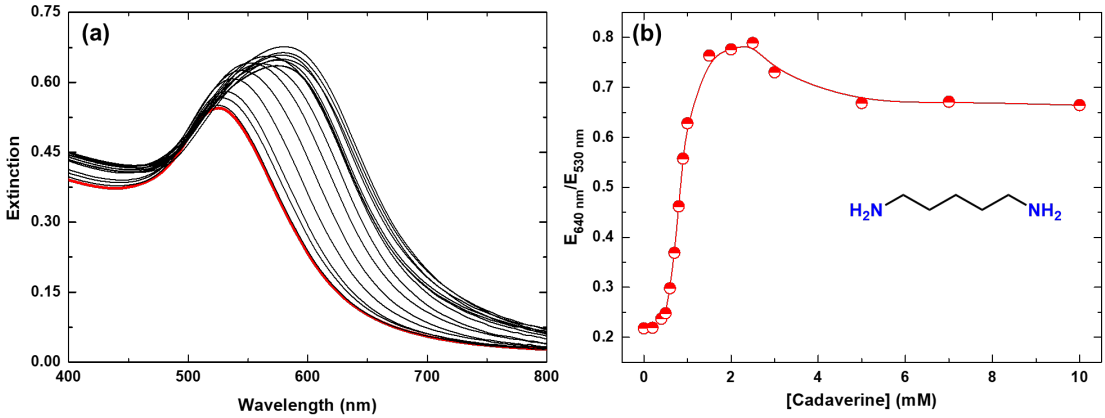

Fig. S23 (a) The extinction spectra and (b) changes in the extinction ratio ($E_{640\ nm}/E_{530\ nm}$) of **S2** (1.2 $\times10^{-4}$ g mL^{-1}) upon the addition of cadaverine in a MES buffer solution (10 mM) at pH 5.5 at 25 °C. [Cadaverine] = 0 − 10 mM.

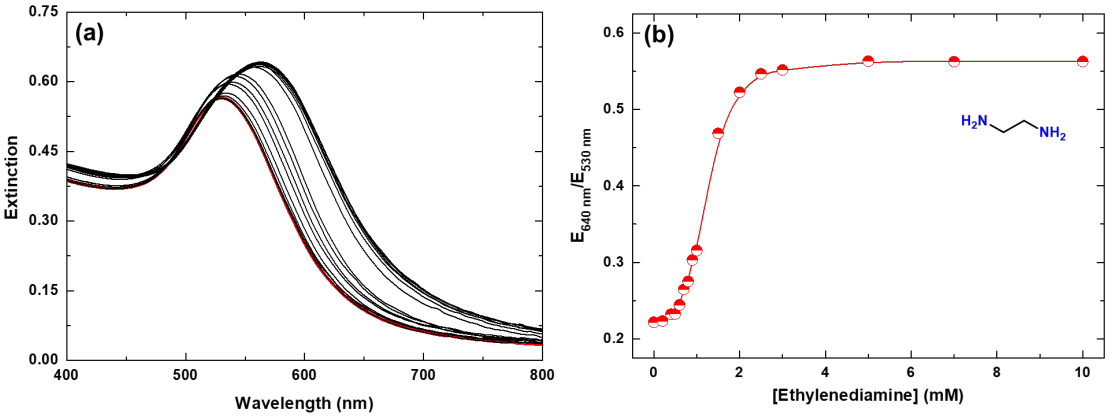

Fig. S24 (a) The extinction spectra and (b) changes in the extinction ratio ($E_{640\ nm}/E_{530\ nm}$) of **S3** (1.2 $\times10^{-4}$ g mL^{-1}) upon the addition of ethylenediamine in a MES buffer solution (10 mM) at pH 5.5 at 25 °C. [Ethylenediamine] = 0 − 10 mM.

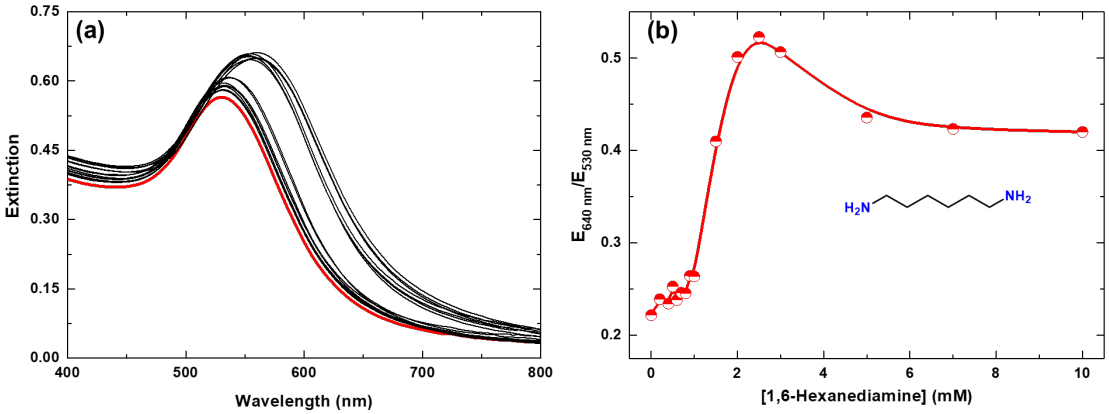

Fig. S25 (a) The extinction spectra and (b) changes in the extinction ratio ($E_{640\ nm}/E_{530\ nm}$) of **S3** (1.2 $\times10^{-4}$ g mL^{-1}) upon the addition of 1,6-hexanediamine in a MES buffer solution (10 mM) at pH 5.5 at 25 °C. [1,6-Hexanediamine] = 0 − 10 mM.

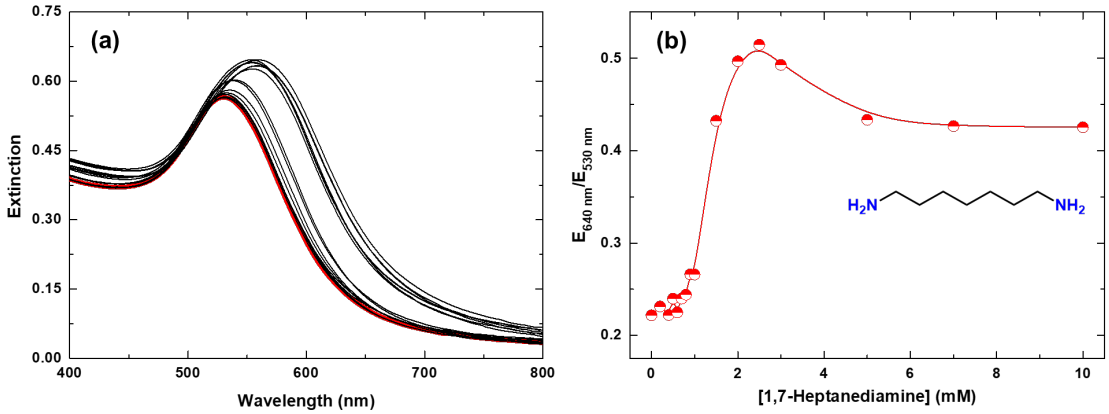

Fig. S26 (a) The extinction spectra and (b) changes in the extinction ratio ($E_{640\ nm}/E_{530\ nm}$) of **S3** (1.2 $\times10^{-4}$ g mL^{-1}) upon the addition of 1,7-heptanediamine in a MES buffer solution (10 mM) at pH 5.5 at 25 °C. [1,7-Heptanediamine] = 0 − 10 mM.

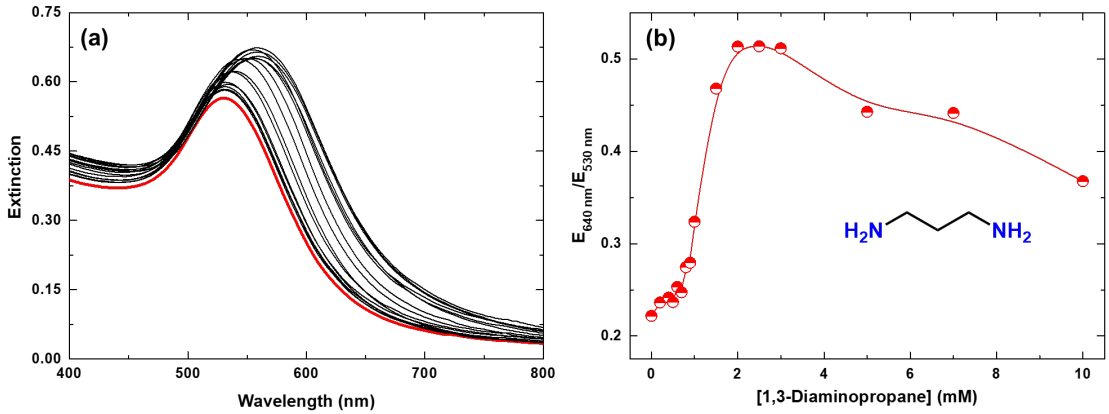

Fig. S27 (a) The extinction spectra and (b) changes in the extinction ratio ($E_{640\ nm}/E_{530\ nm}$) of **S3** (1.2 $\times10^{-4}$ g mL^{-1}) upon the addition of 1,3-diaminopropane in a MES buffer solution (10 mM) at pH 5.5 at 25 °C. [1,3-Diaminopropane] = 0 − 10 mM.

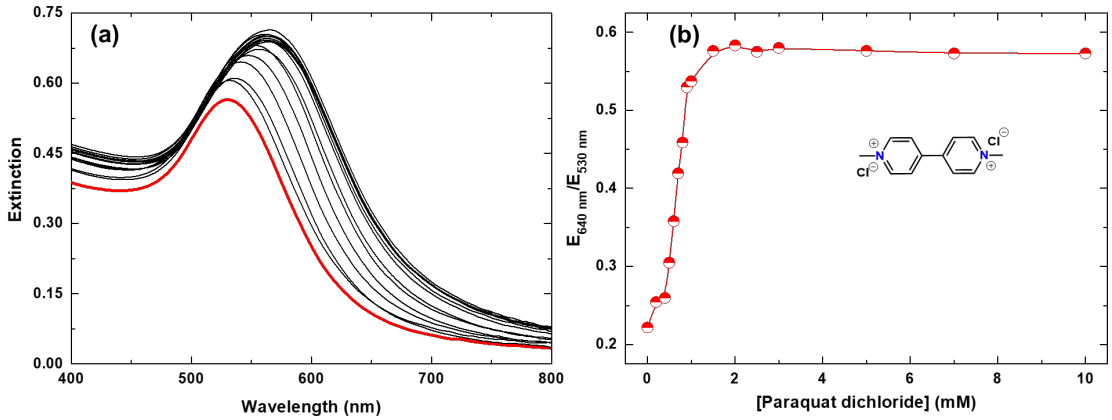

Fig. S28 (a) The extinction spectra and (b) changes in the extinction ratio ($E_{640\ nm}/E_{530\ nm}$) of **S3** (1.2 $\times10^{-4}$ g mL^{-1}) upon the addition of paraquat dichloride in a MES buffer solution (10 mM) at pH 5.5 at 25 °C. [Paraquat dichloride] = 0 − 10 mM.

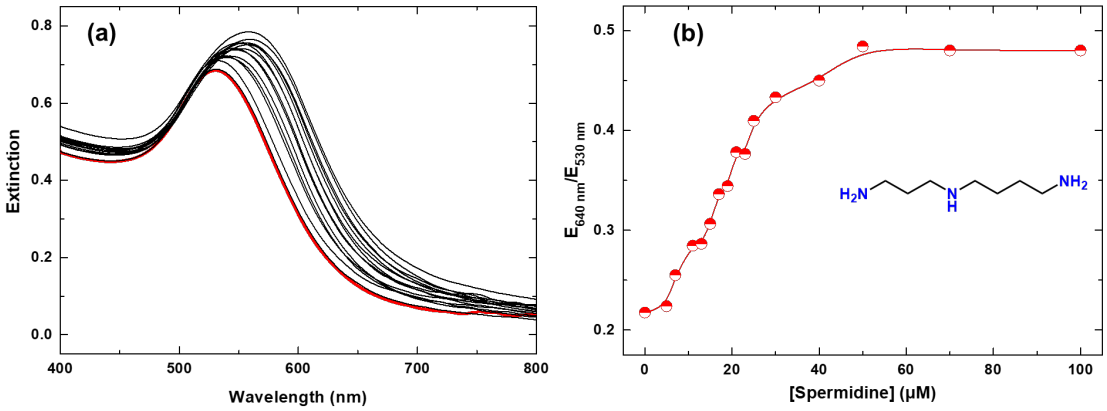

Fig. S29 (a) The extinction spectra and (b) changes in the extinction ratio ($E_{640\ nm}/E_{530\ nm}$) of **S3** (1.2 $\times10^{-4}$ g mL^{-1}) upon the addition of spermidine in a MES buffer solution (10 mM) at pH 5.5 at 25 °C. [Spermidine] = 0 − 100 μM.

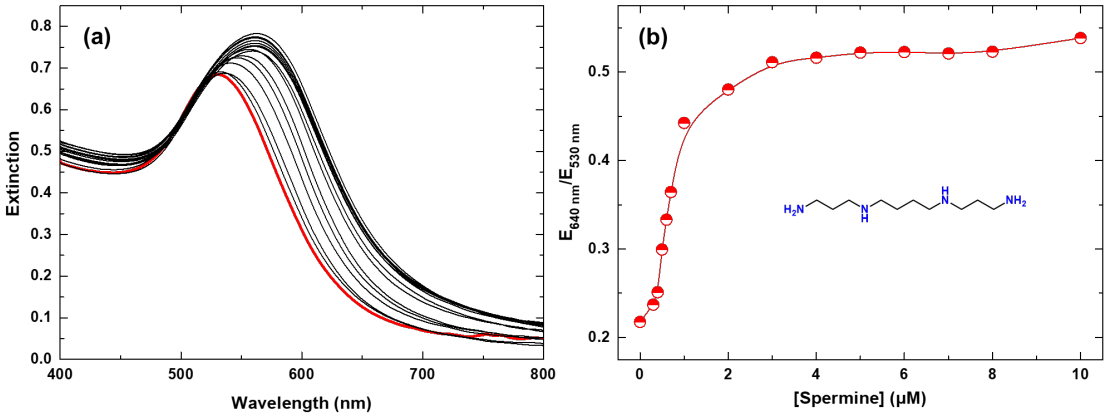

Fig. S30 (a) The extinction spectra and (b) changes in the extinction ratio ($E_{640\ nm}/E_{530\ nm}$) of **S3** (1.2 $\times10^{-4}$ g mL^{-1}) upon the addition of spermine in a MES buffer solution (10 mM) at pH 5.5 at 25 °C. [Spermine] = 0 − 10 μM.

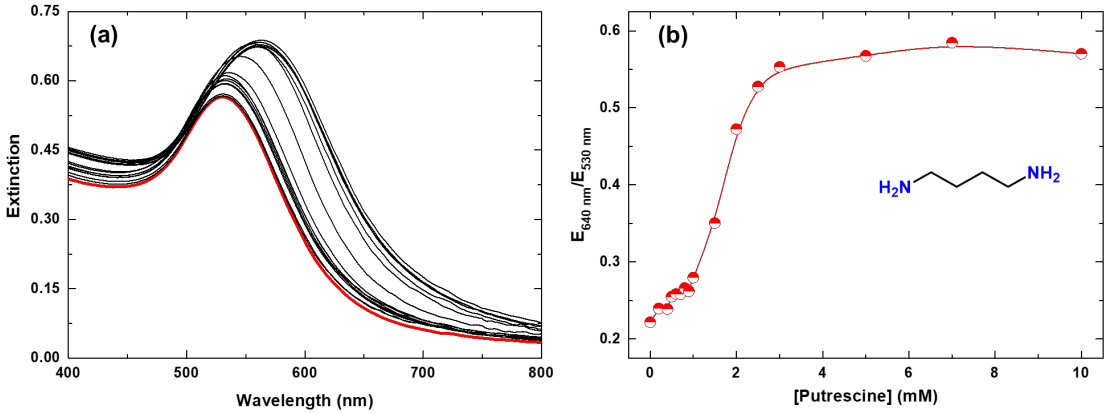

Fig. S31 (a) The extinction spectra and (b) changes in the extinction ratio ($E_{640\ nm}/E_{530\ nm}$) of **S3** (1.2 $\times10^{-4}$ g mL^{-1}) upon the addition of putrescine in a MES buffer solution (10 mM) at pH 5.5 at 25 °C. [Putrescine] = 0 − 10 mM.

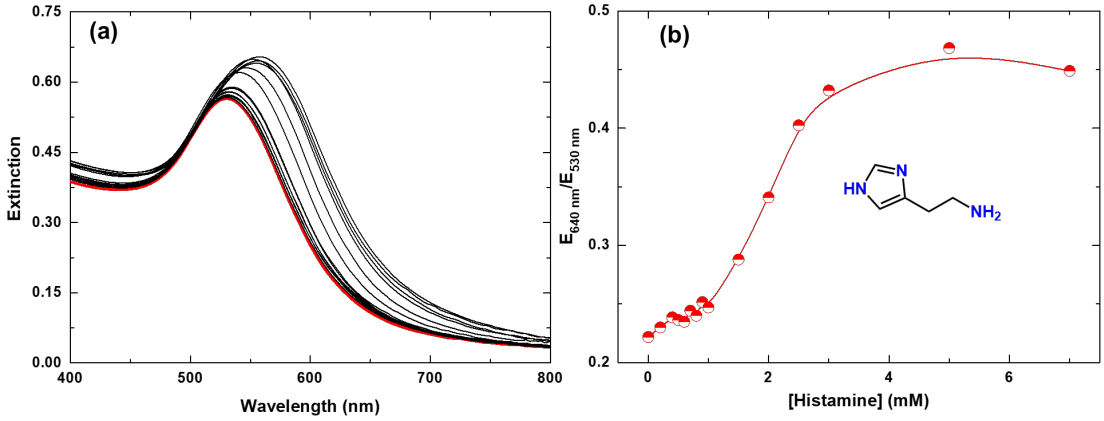

Fig. S32 (a) The extinction spectra and (b) changes in the extinction ratio ($E_{640\ nm}/E_{530\ nm}$) of **S3** (1.2 $\times10^{-4}$ g mL^{-1}) upon the addition of histamine in a MES buffer solution (10 mM) at pH 5.5 at 25 °C. [Histamine] = 0 – 7 mM.

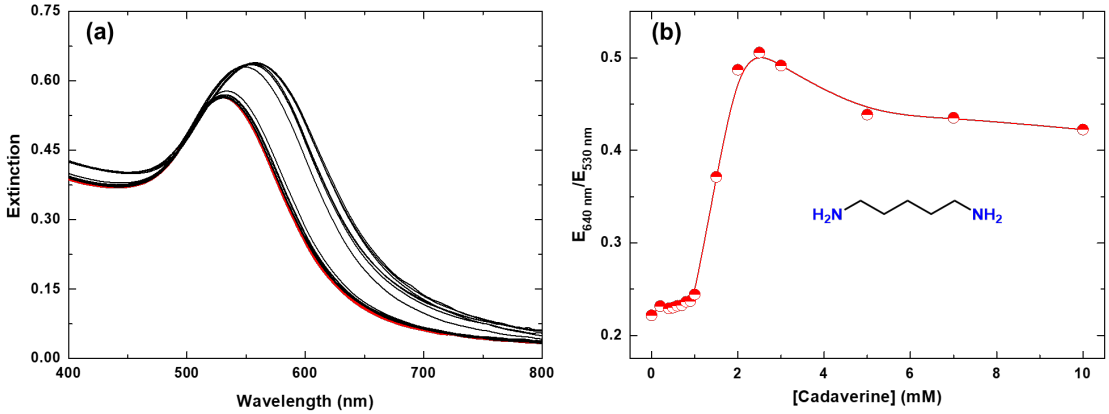

Fig. S33 (a) The extinction spectra and (b) changes in the extinction ratio ($E_{640\ nm}/E_{530\ nm}$) of **S3** (1.2 $\times10^{-4}$ g mL^{-1}) upon the addition of cadaverine in a MES buffer solution (10 mM) at pH 5.5 at 25 °C. [Cadaverine] = 0 – 10 mM.

3-4. Selectivity test

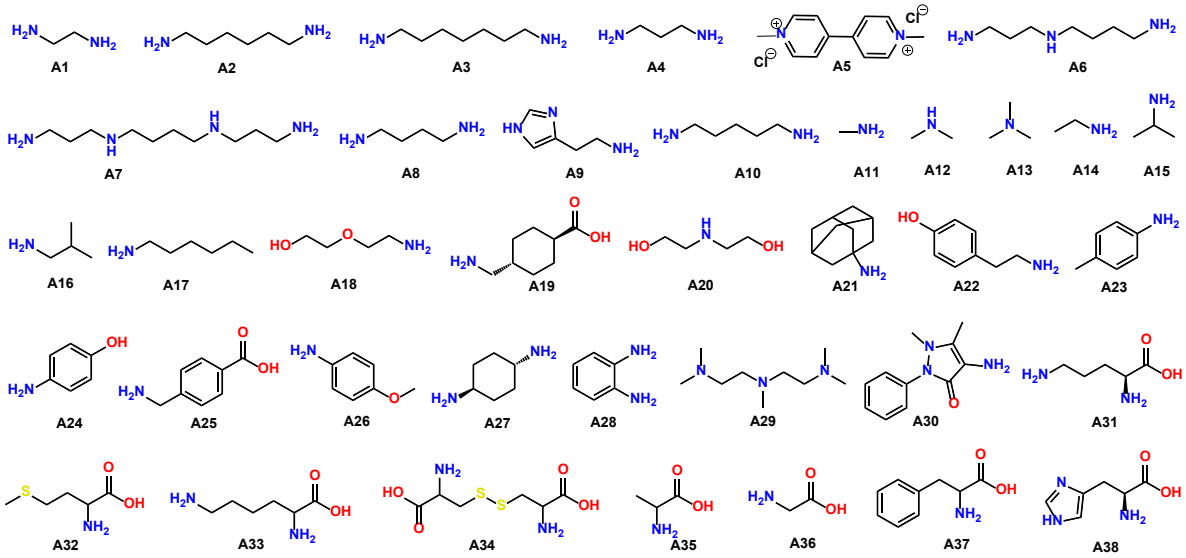

Fig. S34 List of target amines for the selectivity test.

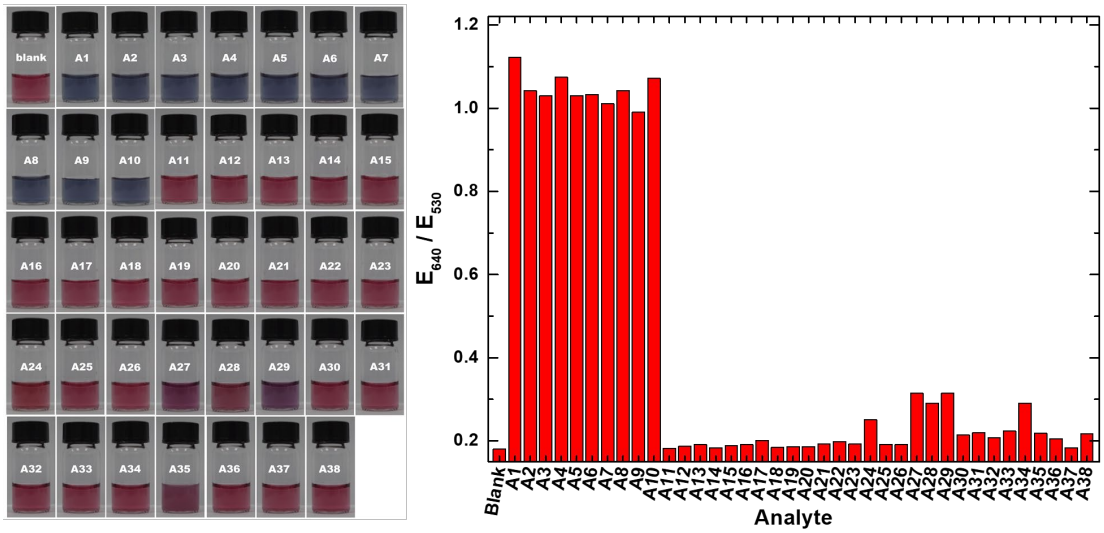

Fig. S35 (a) Photographs of **S1** (1.2×10^{-4} g mL^{-1}) and with analytes. (b) Changes in the extinction ratio ($E_{640\ nm}/E_{530\ nm}$) of **S1** upon the addition of analytes in a MES buffer solution (10 mM) at pH 5.5 at 25 °C. [Analyte] = 3 mM.

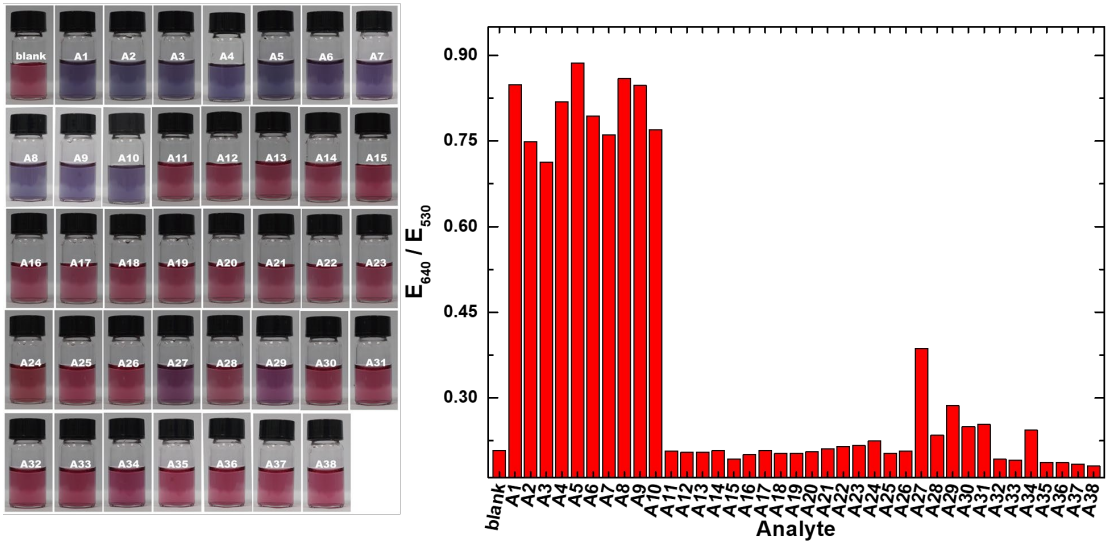

Fig. S36 (a) Photographs of **S2** (1.2×10^{-4} g mL^{-1}) and with analytes. (b) Changes in the extinction ratio ($E_{640\ nm}/E_{530\ nm}$) of **S2** upon the addition of analytes in a MES buffer solution (10 mM) at pH 5.5 at 25 °C. [Analyte] = 3 mM.

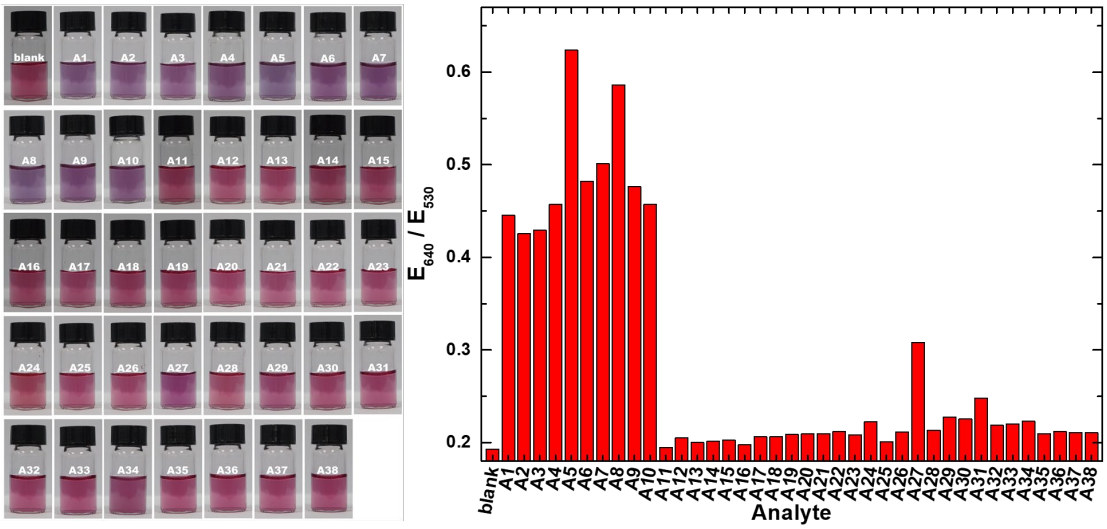

Fig. S37 (a) Photographs of **S3** (1.2×10^{-4} g mL^{-1}) and with analytes. (b) Changes in the extinction ratio ($E_{640\ nm}/E_{530\ nm}$) of **S3** upon the addition of analytes in a MES buffer solution (10 mM) at pH 5.5 at 25 °C. [Analyte] = 3 mM.

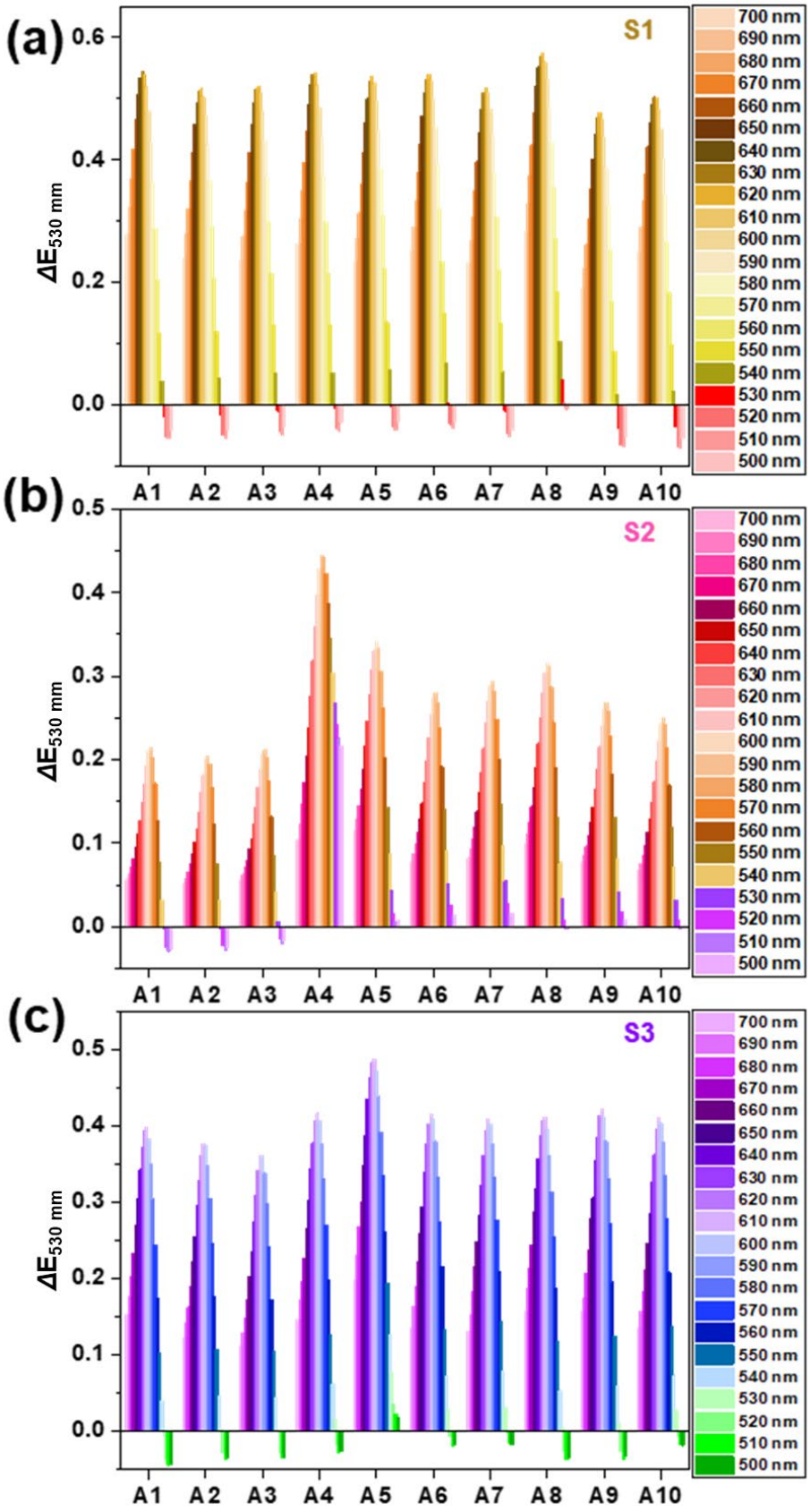

Fig. S38 Cross-reactive response pattern generated by **S1**, **S2** and **S3** using 41 wavelengths in the presence of amines (**A1**–**A10**) in a MES buffer solution (10 mM) at pH 5.5 at 25 °C. [**S1**–**S3**] = 1.2 ×10^{-4} g mL^{-1}, [analyte] = 3 mM.

4. Evaluation of AuNP-based chemosensors with amines

4-1. Field emission scanning electron microscopy (FE-SEM)

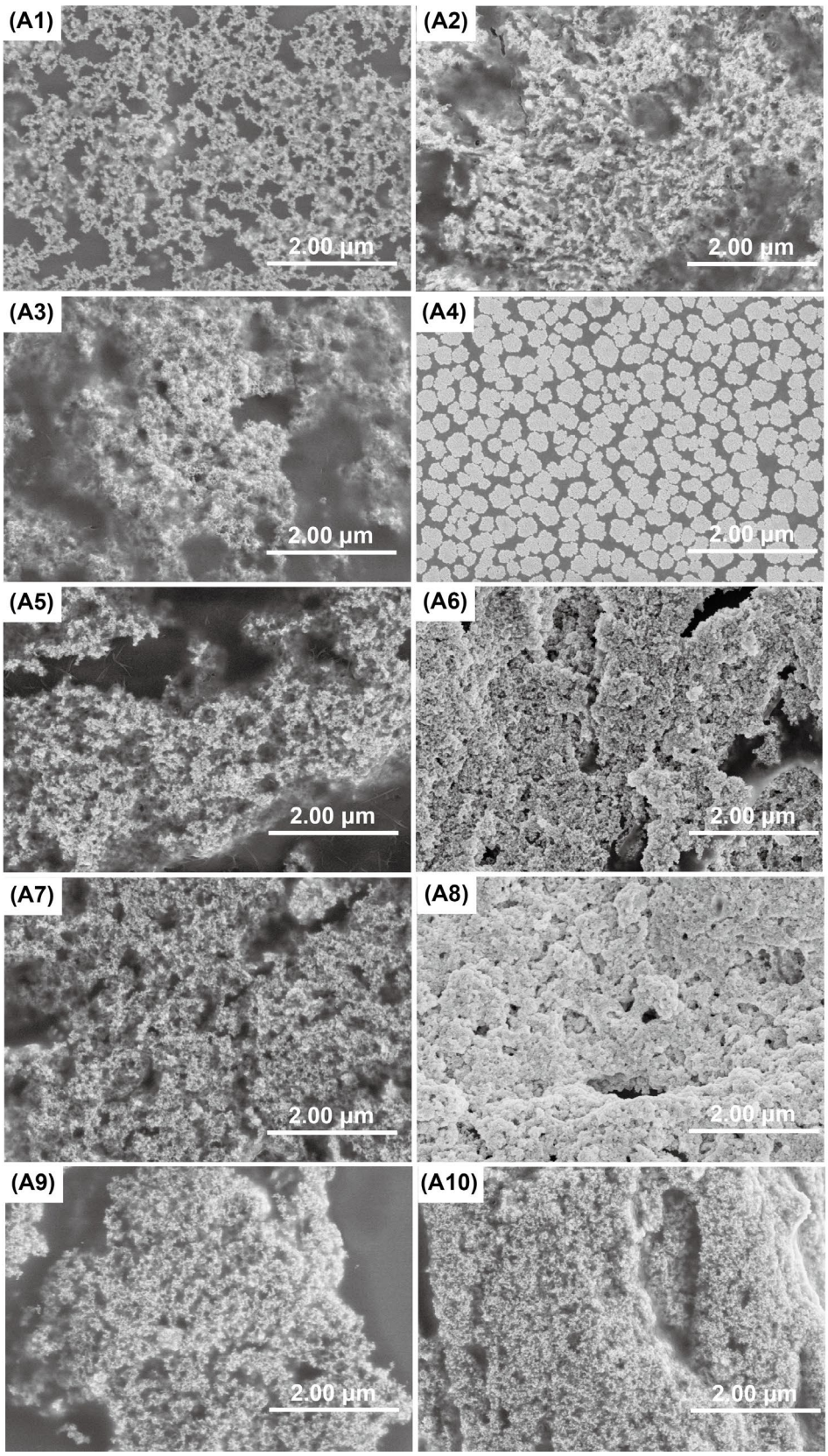

Fig. S39 The FE-SEM microphotographs of **S2** after adding different analytes.

4-2. Dynamic light scattering (DLS)

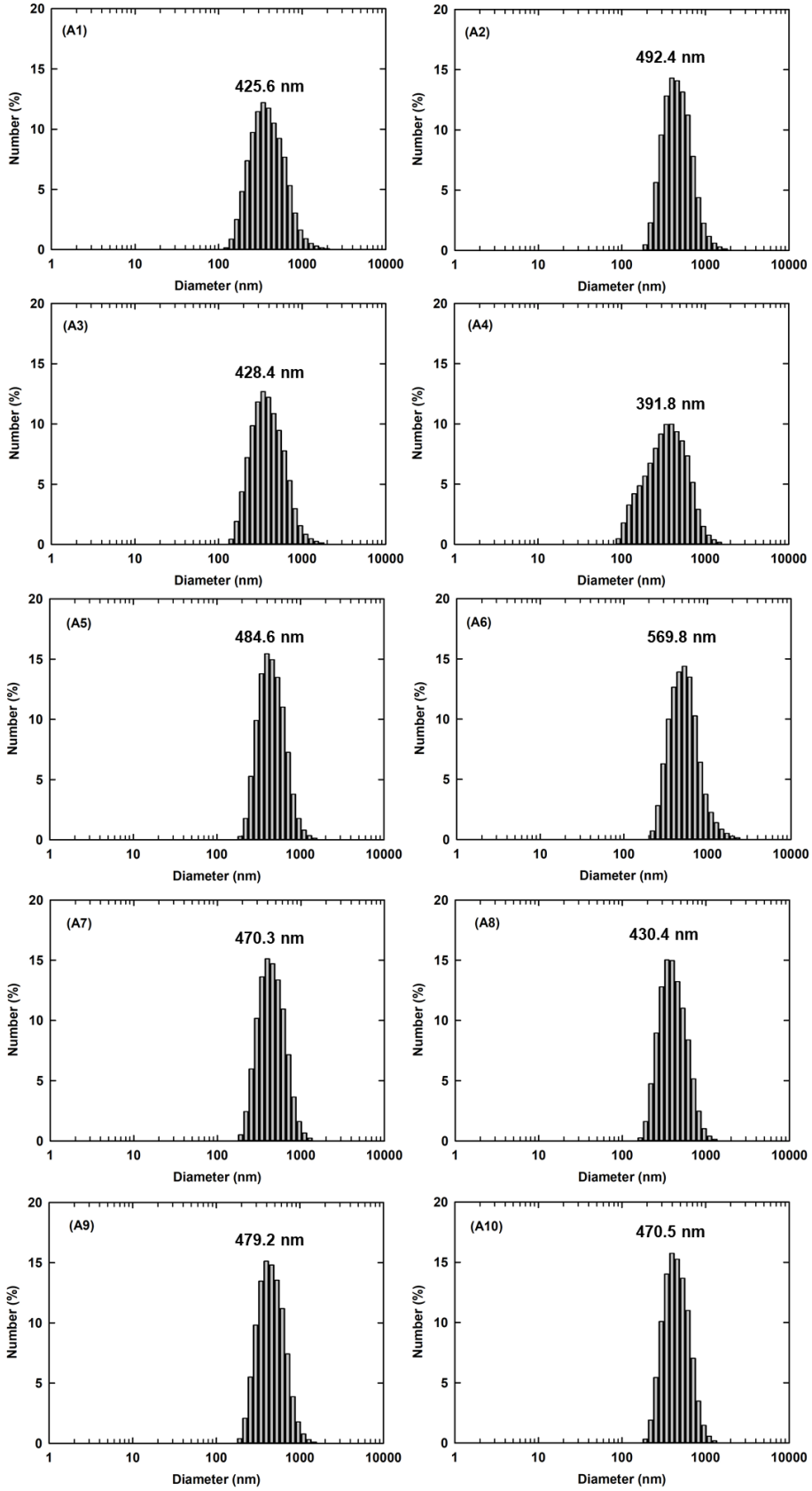

Fig. S40 The DLS diameter histogram of **S2** after adding different analytes (blank, **A1**–**A10**). [Analyte] = 3 mM.

4-3. Zeta potential

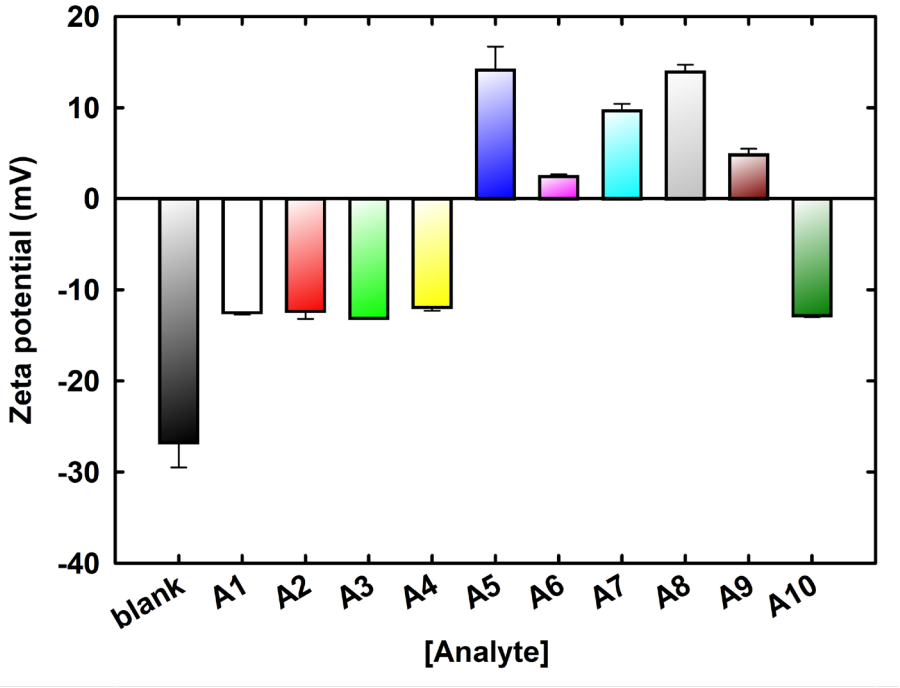

Fig. S41 The Zeta potential of **S2** after adding different analytes (blank, **A1**–**A10**). [Analyte] = 3 mM. All experiments were repeated three times.

4-4. Elemental analysis

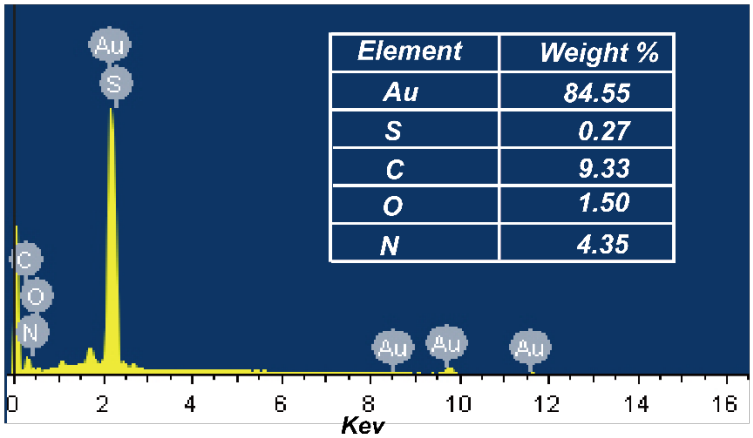

Fig. S42 The EDX profile of **S2** after adding **A9**.

5. Array experiments

5-1. General procedure

The array experiments for qualitative and quantitative analyses were performed in 96-well microplates using a Beckman BioRAPTR microfluidic robotic dispenser. The fluids [MES buffer (10 mM) at pH 5.5 at 25 °C], AuNP sensors (**S1**–**S3**) (1.2×10^{-4} g mL^{-1}), and analyte solutions were contact-free dispensed as follows. Each experiment was performed in 24 repetitions. Each well received 135 µL of the buffer solution containing the sensors. Subsequently, 15 µL of analyte solutions or water were

dispensed. After this period, all extinction spectra of the AuNPs in the 96-well microplate were recorded within 20 min. Extinction spectra of the chemosensors were recorded from 400 nm to 800 nm by using a Tecan infinite 200 microplate reader.

5-2. Linear discriminant analysis (LDA)

Qualitative assay

Table S1 The jackknifed classification matrix of qualitative assay.

	A1	A2	A3	A4	A5	A7	A8	A9	A10	A6	control	%correct
A1	20	0	0	0	0	0	0	0	0	0	0	100
A2	0	20	0	0	0	0	0	0	0	0	0	100
A3	0	0	20	0	0	0	0	0	0	0	0	100
A4	0	0	0	20	0	0	0	0	0	0	0	100
A5	0	0	0	0	20	0	0	0	0	0	0	100
A7	0	0	0	0	0	20	0	0	0	0	0	100
A8	0	0	0	0	0	0	20	0	0	0	0	100
A9	0	0	0	0	0	0	0	20	0	0	0	100
A10	0	0	0	0	0	0	0	0	20	0	0	100
A6	0	0	0	0	0	0	0	0	0	20	0	100
control	0	0	0	0	0	0	0	0	0	0	20	100
Total	20	20	20	20	20	20	20	20	20	20	20	100

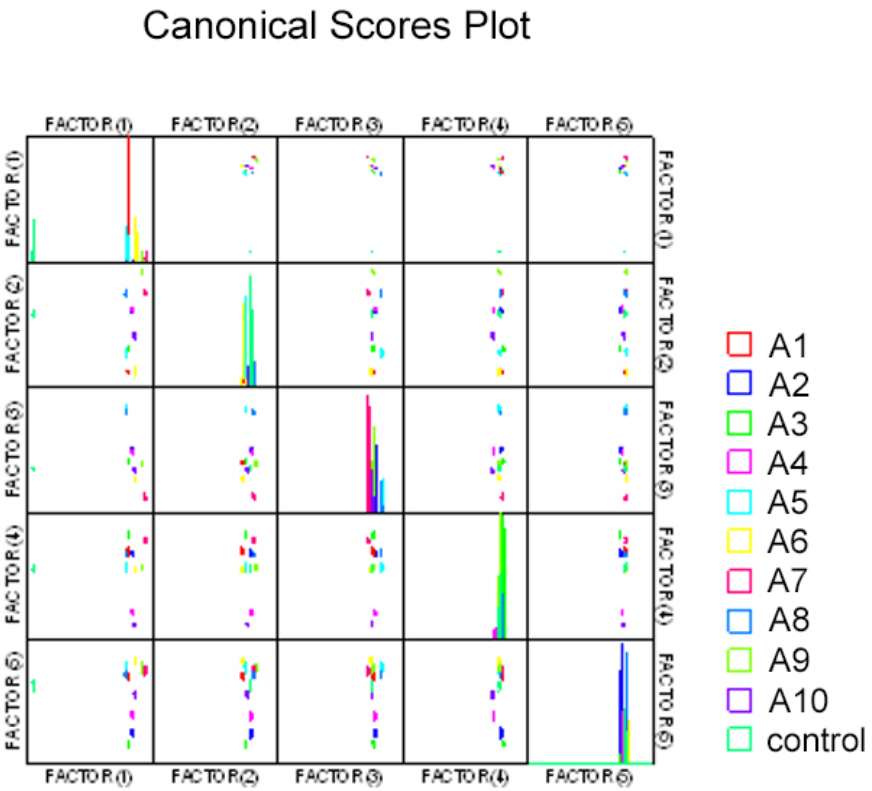

Fig. S43 The canonical scores plot of qualitative assay.

Semi-quantitative assay

Table S2 The jackknifed classification matrix of semi-quantitative assay.

	A7-0.1 μM	**A7**-0.2 μM	**A7**-0.3 μM	**A7**-0.4 μM	**A7**-0.5 μM	**A9**-0.6 mM	**A9**-0.7 mM	**A9**-0.9 mM	**A9**-1.2 mM	**A9**-2.0 mM
A7-0.1 μM	20	0	0	0	0	0	0	0	0	0
A7-0.2 μM	0	20	0	0	0	0	0	0	0	0
A7-0.3 μM	0	0	20	0	0	0	0	0	0	0
A7-0.4 μM	0	0	0	20	0	0	0	0	0	0
A7-0.5 μM	0	0	0	0	20	0	0	0	0	0
A9-0.6 mM	0	0	0	0	0	20	0	0	0	0
A9-0.7 mM	0	0	0	0	0	0	20	0	0	0
A9-0.9 mM	0	0	0	0	0	0	0	20	0	0
A9-1.2 mM	0	0	0	0	0	0	0	0	20	0
A9-2.0 mM	0	0	0	0	0	0	0	0	0	20
A6-10 μM	0	0	0	0	0	0	0	0	0	0
A6-15 μM	0	0	0	0	0	0	0	0	0	0
A6-3.0 μM	0	0	0	0	0	0	0	0	0	0
A6-5.0 μM	0	0	0	0	0	0	0	0	0	0
A6-7.0 μM	0	0	0	0	0	0	0	0	0	0
control	0	0	0	0	0	0	0	0	0	0
Total	20	20	20	20	20	20	20	20	20	20

Jackknifed Classification Matrix							
	A6-10 μM	**A6**-15 μM	**A6**-3.0 μM	**A6**-5.0 μM	**A6**-7.0 μM	control	%correct
A7-0.1 μM	0	0	0	0	0	0	100
A7-0.2 μM	0	0	0	0	0	0	100
A7-0.3 μM	0	0	0	0	0	0	100
A7-0.4 μM	0	0	0	0	0	0	100
A7-0.5 μM	0	0	0	0	0	0	100
A9-0.6 μM	0	0	0	0	0	0	100
A9-0.7 mM	0	0	0	0	0	0	100
A9-0.9 mM	0	0	0	0	0	0	100
A9-1.2 mM	0	0	0	0	0	0	100
A9-2.0 mM	0	0	0	0	0	0	100
A6-10 μM	20	0	0	0	0	0	100
A6-15 μM	0	20	0	0	0	0	100
A6-3.0 μM	0	0	20	0	0	0	100
A6-5.0 μM	0	0	0	20	0	0	100
A6-7.0 μM	0	0	0	0	20	0	100
control	0	0	0	0	0	20	100
Total	20	20	20	20	20	20	100

5-3. Regression analysis in mixtures: support vector machine (SVM)

Table S3 Concentration conditions in the quantitative assay of the mixtures. The gray lines mean validation data sets while other lines mean calibration data sets. All measurements were carried out in a MES buffer solution (10 mM) at pH 5.5 at 25 °C.

Histamine (mM)	Spermine (μM)	Spermidine (μM)
0.50	0.300	10.0
0.45	0.250	9.0
0.40	0.200	8.0
0.35	0.175	7.0
0.30	0.150	6.0
0.25	0.125	5.0
0.20	0.100	4.0
0.15	0.075	3.0
0.10	0.050	2.0
0.05	0.025	1.0
0	0	0

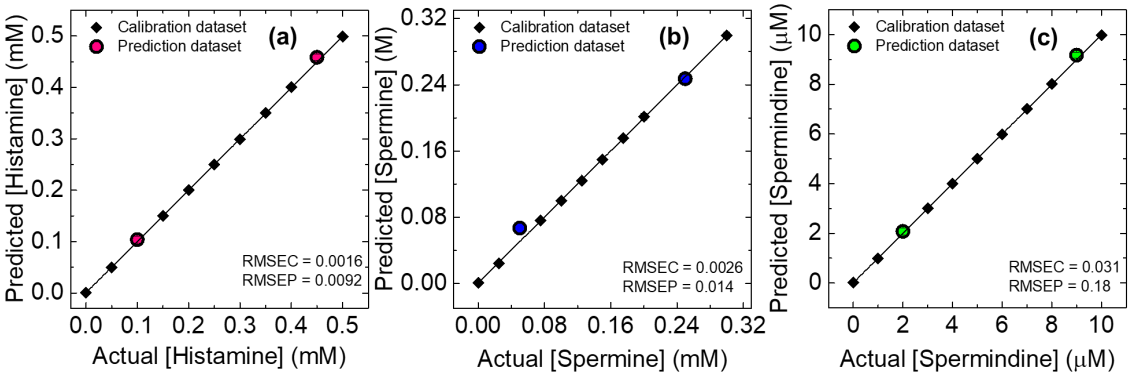

Fig. S44 The results of regression analysis of (a) histamine, (b) spermine, and (c) spermidine in the mixtures. The values of the root mean-square of calibration (RMSEC) and prediction (RMSEP) prove high accuracies of the model and its predictive capacity.

6. Raw fish analysis

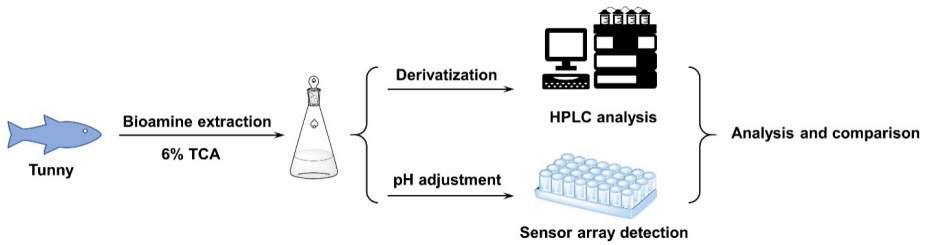

Fig. S45 Schematic illustration of the extraction process of amines from the raw fish.

6-1. High performance liquid chromatography (HPLC) analysis

Table S4 Gradient elution program for biogenic amines analysis.

Time / min	0	5	20	24	25	30	60
Water / %	65	70	100	100	100	65	65
Acetonitrile /%	35	30	0	0	0	35	35

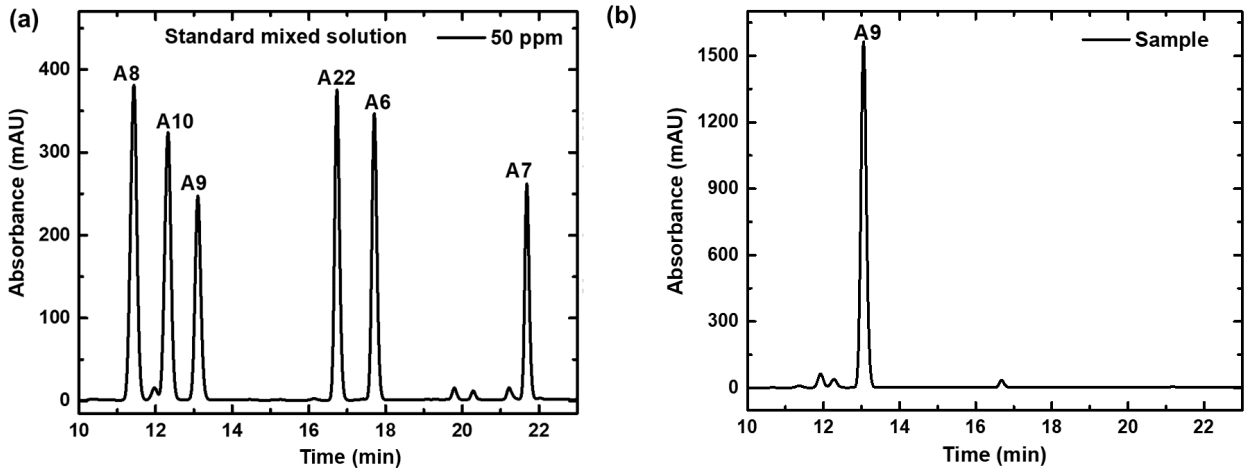

Fig. S46 The adsorption spectrum of (a) the standard mixed solution and (b) the extracted sample from the fish (tuna) stored for 24 h at 25 °C. The 60 times diluted sample was used in this test.

7-2. Real sample analysis using the chemosensor array

Table S5 Comparison table for HPLC and the chemosensor array.

Time (h)	Histamine (μM)		
	HPLC	**Sensor array**	Accuracy (%)
24	44.8	38.3±0.6	85.6
48	66.5	69.6±1.7	104.6
72	99.7	96.9±2.0	97.1